The effect of confinement on the temperature dependence of the excitonic transition energy in GaAs/$Al_xGa_{1-x}As$ quantum wells

2008 J. Phys.: Condens. Matter 20 255246

(http://iopscience.iop.org/0953-8984/20/25/255246)

J. Phys.: Condens. Matter **20** (2008) 255246 (9pp) doi:10.1088/0953-8984/20/25/255246

The effect of confinement on the temperature dependence of the excitonic transition energy in GaAs/$Al_xGa_{1-x}As$ quantum wells

M A T da Silva[1], R R O Morais[1], I F L Dias[1], S A Lourenço[1], J L Duarte[1], E Laureto[1], A A Quivy[2] and E C F da Silva[2]

[1] Departamento de Física, Universidade Estadual de Londrina UEL, CP6001, CEP 86051-970, Londrina, Paraná, Brazil
[2] Instituto de Física, Universidade de São Paulo, CP66318, CEP 05315-970, São Paulo, SP, Brazil

Received 22 February 2008
Published 27 May 2008
Online at stacks.iop.org/JPhysCM/20/255246

Abstract

We determined by means of photoluminescence measurements the dependence on temperature of the transition energy of excitons in GaAs/$Al_xGa_{1-x}As$ quantum wells with different alloy concentrations (with different barrier heights). Using a fitting procedure, we determined the parameters which describe the behavior of the excitonic transition energy as a function of temperature according to three different theoretical models. We verified that the temperature dependence of the excitonic transition energy does not only depend on the GaAs material but also depends on the barrier material, i.e. on the alloy composition. The effect of confinement on the temperature dependence of the excitonic transition is discussed.

1. Introduction

The band-gap energy of semiconductor materials and its dependence on temperature are known to be among the most important parameters for the development of devices operating with well defined specifications (desirable spectral range, stability of operation at elevated temperatures, high speed, among other electronic, optical, and mechanical properties). The temperature dependence of the energy gap (E_g) has a different behavior in different ranges of temperature. At very low temperatures ($T < 0.02\ \Theta_D$, where Θ_D is the Debye temperature) $E_g(T)$ has asymptotic behavior proportional to T^4 as $T \to 0$ [1, 2]. With increasing temperature, the behavior of $E_g(T)$ can be represented by a T^p dependence where p has values in the range $2 < p < 3.33$ [3]. At higher temperatures the energy gap decreases linearly with increasing temperatures [1–3].

In general, the dependence on temperature of E_g is determined by two different mechanisms: the electron–phonon interaction and the thermal expansion of the lattice [4–7]. To many semiconductor materials, the contribution of the thermal expansion of the lattice is a minor effect in the behavior of $E_g(T)$ as compared to the electron–phonon interaction [7, 8]. For this reason, several models describing the dependence on temperature of $E_g(T)$ were proposed in the literature just taking into account the electron–phonon interaction [9]. Among the models usually used to describe $E_g(T)$ we find the semi-empirical models which take into account the electron–phonon interaction and use the Bose–Einstein statistics as proposed by Manoogian and Leclerc [10], the model of Viña and collaborators [11], the more recent analytical models proposed by Pässler [12], or the empirical relation proposed by Varshni [13].

In $Al_xGa_{1-x}As$ bulk material, the adjustable parameters of different models describing $E_g(T)$—especially the set of parameters (α_i, Θ_i) where $\alpha_i \equiv -(dE/dT)_{T\to\infty} \equiv S(\infty)$ is the high-temperature limiting value of the forbidden gap entropy and Θ_i is the phonon energy in units of the absolute temperature—are dependent on the aluminum concentration (x) showing an increasing behavior with increase of Al concentration in the composition range $0 < x < 0.45$ [14, 15]. As far as GaAs/$Al_xGa_{1-x}As$ quantum well (QW) heterostructures are concerned, Lourenço *et al* [16, 17] verified that the aluminum concentration of the barrier material

has influence on the temperature dependence of the excitonic transition energy. The values of the fitting parameters associated to different models describing the behavior of $E_g(T)$ decrease with the introduction of the barriers but increase as the Al concentration increases [18]. This decrease of the values of the fitting parameters with increasing T was attributed to the transition from the three-dimensional (3D) to the two-dimensional (2D) confinement condition [16, 17]. The same trend is also observed in the behavior of the parameter related to the contribution of exciton–acoustic phonon interaction used to fit experimentally measured line widths by resonant Raman scattering, absorption, and photoluminescence (PL) spectroscopy [19–25].

Since the energy of the LO-phonons and the strength of the exciton–LO-phonon interaction increase with the Al concentration, a larger line width of the excitonic emission and also a pronounced variation of $E_g(T)$ is expected (being more pronounced for $T > 150$ K). In the region of low temperatures, the exciton–phonon interaction is determined by the LA-phonons, which do not depend on the Al concentration [19]. In this way, if we analyze the behavior of $E_g(T)$ in the low temperature range ($9 \leqslant T \leqslant 100$ K) for the GaAs bulk material and also for the GaAs/Al_xGa_{1-x}As QWs for different values of the Al concentration, it is possible to obtain information about the influence of the alloy composition on the fitting parameters and by comparing the results obtained for the 3D system (GaAs bulk) and the 2D systems (GaAs/GaAlAs QWs) we will be able to obtain information about the influence of the confinement on the temperature dependence of the band-gap energy. We will also be able to obtain information about the electron–acoustic phonon interaction. Due to their specificities, the models used to describe $E_g(T)$ have different susceptibilities with regard to the electron–phonon interaction associated to the acoustic (TA, LA) and optical (TO, LO) phonon branches. As a consequence, it is necessary to make a systematic comparison among the results obtained with the different models in order to obtain information about the dependence of the fitting parameters of $E_g(T)$ on confinement effects.

In the present work we studied the behavior of the energy gap (more precisely, the excitonic transition energy) as a function of temperature be means of PL measurements. Using a fitting procedure, we determined the parameters which describe the behavior of the exciton energy as a function of temperature according to three different theoretical models as proposed by Viña and Pässler. By comparing the results of the fits obtained for the GaAs bulk material and GaAs/AlGaAs QWs, the influence of the aluminum concentration and the effect of the confinement on the behavior of the fitting parameters were determined.

2. Theoretical fitting models

In this section we present the different expressions used to analyze the dependence of E_g with temperature. The expression proposed by Viña *et al* is given by [11]:

$$E_g(T) = E_B - a_B\left[1 + \frac{2}{\exp(\Theta_B/T) - 1}\right] \tag{1}$$

where $E_g(T = 0\ \text{K}) = E_B - a_B$ is the energy gap at $T = 0$ K, a_B represents the strength of the electron–phonon interaction, and $\Theta_B \equiv h\omega/k_B$ is the characteristic temperature representing the effective phonon energy on the temperature scale. For future comparison of the fitting parameters obtained according to the three different models used in this work, it is convenient to introduce here the parameter α_B defined as $\alpha_B \equiv -(dE/dT)_{T\to\infty} = 2a_B/\Theta_B$ which is the limit of the gap shrinkage coefficient that can be determined by the slope of $E_g(T)$ versus T as $T \to \infty$. We also used in the present work two different models developed by Pässler (here named p-type and ρ-type models) [13, 26]. The expression describing $E_g(T)$ according to the p-type model is given by:

$$E_g(T) = E_g(0) - \frac{\alpha_p\Theta_p}{2}\left[\sqrt[p]{1 + \left(\frac{2T}{\Theta_p}\right)^p} - 1\right] \tag{2}$$

where $E_{g(0)}$ is the energy gap at $T = 0$ K, α_p is the high-temperature limit slope of the gap $-(dE_g(T)/dT)_{T\to\infty}$, Θ_p is the phonon energy in units of the absolute temperature, and p is an empirical parameter related to the shape of the electron–phonon spectral function by the relation:

$$f(\omega) = \begin{cases} \nu\left(\dfrac{\alpha}{k_B}\right)\left(\dfrac{\omega}{\omega_0}\right)^{\nu} & \text{to } \omega < \omega_0 \\ 0 & \text{to } \omega > \omega_0 \end{cases} \tag{3}$$

where the ω_0 is the cutoff frequency and can be determined by the fitting procedure using the relation $\hbar\omega_0 = [(\nu+1)/\nu]k_B\Theta_p = [p/(p-1)]k_B\Theta_p$ with $p = \nu + 1$. The dispersion of this model is given by $\Delta p \equiv 1/\sqrt{p^2-1}$. According to the ρ-type model, $E_g(T)$ is described by the expression:

$$E_g(T) = E_\rho - \frac{\alpha_\rho\Theta_\rho}{2} \times \left[\frac{\rho}{2}\left(\sqrt[4]{1 + \frac{\pi^2}{6}\left(\frac{4T}{\Theta_\rho}\right)^2 + \left(\frac{4T}{\Theta_\rho}\right)^4} - 1\right) + (1-\rho)\left(\coth\left(\frac{\Theta_\rho}{2T}\right) - 1\right)\right] \tag{4}$$

where $E_\rho = E_g(T = 0\ \text{K})$ is the energy gap at $T = 0$ K; $\alpha_\rho \equiv -(dE_g(T)/dT)_{T\to\infty}$ and Θ_ρ is the phonon energy in a temperature scale related to the effective phonon energy by the expression, $\Theta_r = \Theta_\rho(1 - \rho/2)$. The empirical parameter ρ describes the relative weight of the contribution of acoustical and optical phonons to the behavior of $E_g(T)$. In the limit of $\rho \to 1$, the interaction is determined by acoustic phonons while in the limit as $\rho \to 0$, optical phonons control the exciton–phonon interaction. The dispersion of this model is described by $\Delta\rho = 1/(2-\rho)\sqrt{(\rho/3)(4-3\rho)}$.

In order to determine the adjustable parameters according to each theoretical expression (equations (1)–(3)) we used a chi-squared fitting procedure. The criterion used to obtain reliable fitting parameters was determined according to the expression:

$$S^2 = \left(\frac{1}{n-m}\right)\sum_{i=1}^{n}\left(E_{gi}^{\text{exp}} - E_{gi}^{\text{cal}}\right)^2 \tag{5}$$

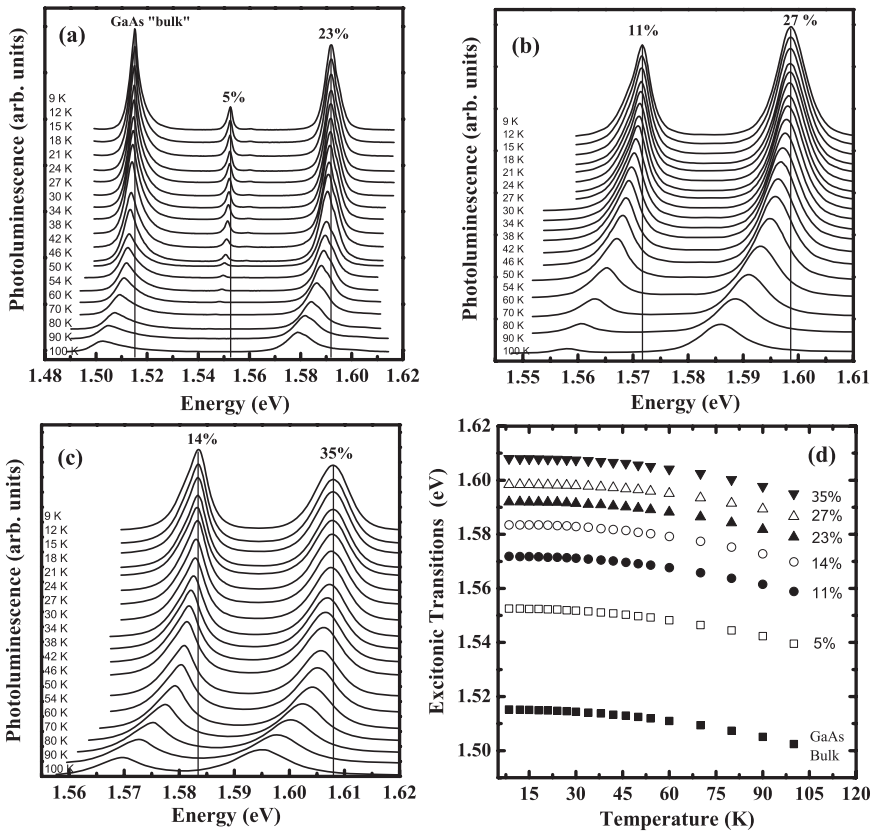

Figure 1. PL spectra as a function of temperature from 9 to 100 K. The numbers in parenthesis indicate the alloy concentrations of the barriers: (a) 5% and 23% for sample #1; (b) 11% and 27% for sample #2; (c) 14% and 35% for sample #3. The vertical dashed lines indicate the energies of the peaks at $T = 9$ K. (d) shows the dependence on temperature of all excitonic transitions observed in the parts (a), (b), and (c).

where $E_{gi}^{\rm exp}(E_{gi}^{\rm cal})$ indicates the experimental (fitted) values of the energy gap for the ith-data point. The factor $(n - m)$ is the number of degrees of freedom left after fitting n data points with m adjustable parameters in the fitting function.

3. Sample and experimental details

The samples here investigated are GaAs/$Al_xGa_{1-x}As$ ($0.05 \leqslant x \leqslant 0.35$) quantum wells grown in a Gen II MBE system on top of epiready semi-insulating GaAs(001) substrates. Each sample has two QWs with 60 Å-nominal well widths which are separated by a 800 Å-thick $Al_xGa_{1-x}As$ barrier. The 800 Å-thick barrier is composed of two 400 Å-thick $Al_xGa_{1-x}As$ layers with two different alloy concentrations being the higher value of x closer to the sample surface. The structure consisted of a 0.1 μm-thick GaAs buffer, a $10 \times (AlAs)_5(GaAs)_{10}$ superlattice, another 0.2 μm-thick GaAs layer, followed by the region of the two 60 Å-thick QWs separated by the 800 Å-AlGaAs barrier. The structures were capped with a 50 Å-GaAs layer.

Photoluminescence measurements were performed in a closed circuit optical cryostat operating with helium from 9 to 100 K. The luminescence signal was analyzed by a monochromator and detected by a GaAs photomultiplier using a standard lock-in technique (Stanford SR 510). In the temperature range $9 \leqslant T \leqslant 30$ K the PL spectra were recorded every 3 K; in the range $30 \leqslant T \leqslant 54$ K measurements were performed every 4 K; and every 10 K in the range $60 \leqslant T \leqslant 100$ K. The density of experimental points is high enough (19 points in the temperature range from 9 to 100 K) to result in a reliable theoretical fit to the data. The experiments were performed with an excitation power of 7 mW (16 W cm^{-2}). Recent studies about the same series of samples showed that this excitation power is enough to screen the effects associated to the alloy fluctuations [27].

4. Results and discussion

Figure 1 shows the PL spectra of each sample for temperatures in the range 9–100 K. The GaAs emission peak observed at 1.515 eV at $T = 9$ K has a full-width at half-maximum of 1.2 meV, indicating the good quality of our samples (see figure 1(a)). The other two peaks observed at higher energies are related to the electron-heavy-hole exciton transition energies related to the two QWs with different barrier compositions. In figure 1(d) is shown the energy of the peaks as a function of temperature for all the emissions observed in figures 1(a)–(c). In figure 2 we show the curves of $E_g(T)$ obtained according to the different theoretical models for sample #3 ($x = 14\%$ and 35% QWs). We observed in our studies that the p-type Pässler model leads to the best fit to

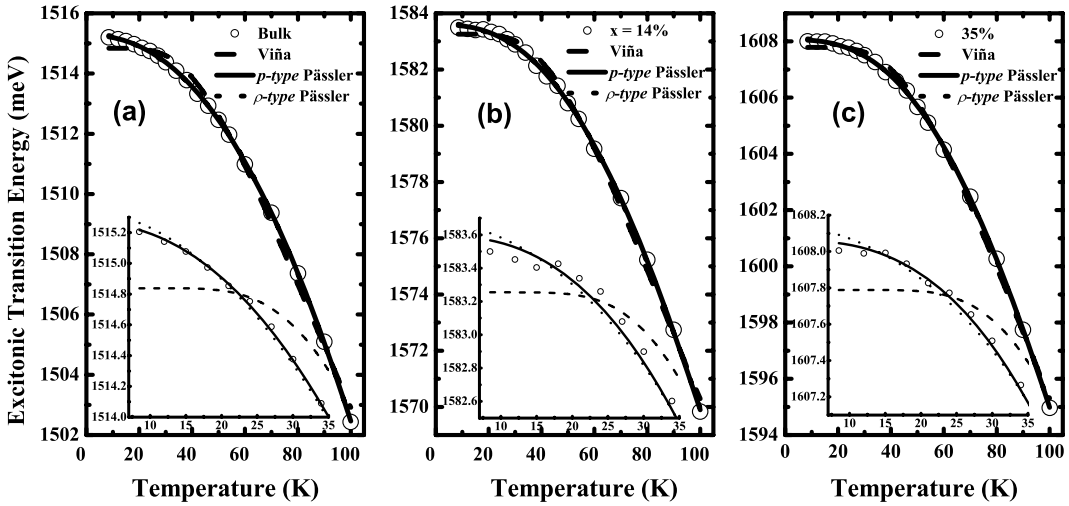

Figure 2. Comparison of the fitted curves obtained for sample #1 with the analytical models of Viña (broken curve), p-type Pässler (full curve), and ρ-type Pässler (dotted curve) for: (a) the GaAs bulk emission peak; (b) the QW with the $Al_{0.14}Ga_{86}As$ barrier; and (c) the QW with the $Al_{0.34}Ga_{65}As$ barrier. The inset shows an enlargement of the 9 to 35 K region of each graphic.

the experimental data, with the smallest values of S^2. The ρ-type Pässler model gives a value for S^2 higher than the p-type model but smaller than the Viña model, which exhibits the well known plateau behavior at low temperatures ($T \leqslant 50$ K). The fitting results for the other two samples show the same trends for the values of S^2.

In figures 3–5 we show the fitted parameters as a function of Al concentration obtained for the six QWs and also for the GaAs according to Viña, p-type, and ρ-type models, respectively, and in table 1 a summary of all the adjusted parameters is presented. We observed from our results that all the parameters related to the energy gap at $T = 0$, $E_B - a_B = E_g(T = 0\ \text{K})$ in the Viña model, E_p in the p-type model, and E_ρ in the ρ-type model, increase with the increase of the barrier heights, i.e. increase with the increase of Al concentration (see figures 3(a), 4(a), and 5(a)). We also observed that the values of the energy gap obtained with the different theoretical expressions do not change so much from model-to-model, and show a similar behavior, which was predicted by theoretical calculations based on the envelope-function approximation for GaAs/AlGaAs QWs [28].

The parameters a_B and Θ_B related to the Viña model do not depend on the presence of the barriers i.e. they are practically constants when the system changes from the 3D (GaAs bulk material) to the 2D (GaAs/GaAlAs QWs) confinement condition: $a_B(x = 0.05) \approx a_B(x = 0.0)$ and $\Theta_B(x = 0.05) \approx \Theta_B(x = 0.0)$, considering the error bars (see figures 3(b) and (d)). Moreover, since the electron–acoustic phonon interaction is prevalent at low temperatures and the typical plateau behavior of $E_g(T)$ for $T \leqslant 50$ K limits the validity of the Viña model in this temperature range, we were expecting a poor description of the physical quantities related to the fitted parameters determined according to this model. However, as can be noticed in our results, the parameters a_B (related to the strength of the electron–phonon interaction) and Θ_B (describing the mean energy of the phonons) systematically increase with the increase of the Al concentration for $x > 0$, showing that the Viña model somehow describes the electron–optical phonon interaction even in a small temperature range ($T < 100$ K). The parameter α_B also increases with the alloy concentration (see figure 3(c)).

The parameters α_p and Θ_p determined according to the p-type model decrease with the 3D-to-2D transition (see figures 4(b) and (d)). Considering the error bars, we can say that these parameters stay approximately constant with the further increase of the alloy concentration, in agreement with the fact that the mean energy of the acoustic phonons does not depend on the alloy concentration. The parameter p increases monotonically with the increase of the alloy concentration from $p(x = 0.0) = 2.2$ to $p(x = 0.35) = 2.8$, indicating a decrease of the dispersion with the increase of x.

The parameters α_ρ and Θ_r determined according to the ρ-type model decrease with the 3D-to-2D transition. For instance, we obtained $\Theta_r(x = 0.05)/\Theta_r(x = 0.0) \cong 1.3$. The parameter α_ρ increases while Θ_r stays constant with a further increase of x. The mean value of Θ_r in the Al-concentration range here considered ($\langle\Theta_r\rangle_x$) varies from 0.05 up to 0.35, values which are superior but approximately equal to the mean value obtained in the p-type model ($\langle\Theta_p\rangle_x$):$\langle\Theta_r\rangle_x = 17$ meV > 16.3 meV $= \langle\Theta_p\rangle_x$. The parameter ρ decreases with the increase of x, showing once again that the electron–optical phonon interaction depends on the chemical composition of the barrier in the temperature range here considered.

The parameters a_B, p, and ρ are characteristics of each model and must be analyzed separately. The intensity of the electron–LO-phonon interaction in quantum wells associated to the a_B parameter can be described by the coupling constant [19, 20, 29]:

$$\lambda = \frac{2\pi e^2 \left(1/\varepsilon_\infty - 1/\varepsilon_s\right)\sqrt{\left(m_e^* + m_h^*\right)\hbar\omega_{LO}/2\hbar^2}}{q^2\Omega} \qquad (6)$$

where ε_∞ and ε_s are the high-frequency and static dielectric constants, m_e* and m_h* are the electron and hole effective

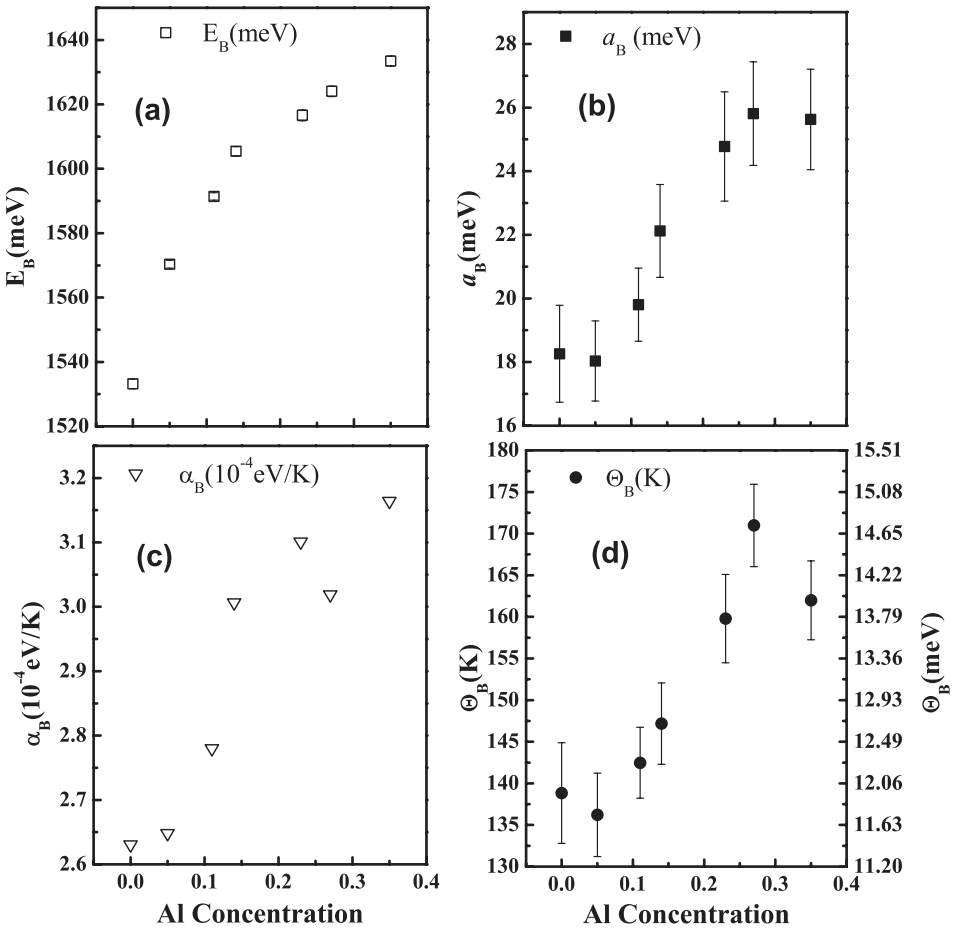

Figure 3. Dependence on aluminum concentration of the fitted parameters according to the Viña model for the temperature range $9 \leqslant T \leqslant 100$ K. The parameter α_B is defined as $\alpha_B \equiv S(T) = -(\mathrm{d}E/\mathrm{d}T)_{T\to\infty} \cong 2a_B/\Theta_B$.

Table 1. Values of the parameters α_i, Θ_i $(i = B, p, r)$, p and ρ (and their respective dispersions) obtained by fitting the dependence of the excitonic recombination energy with temperature in the $9 \leqslant T \leqslant 100$ K for the GaAs bulk material and GaAs/$Al_xGa_{1-x}As$ $(0.05 \leqslant x \leqslant 0.35)$ QWs according to different theoretical models (see equations (1), (2), and (3)).

x	α_B (10^{-4} eV K^{-1})	α_p (10^{-4} eV K^{-1})	α_ρ (10^{-4} eV K^{-1})	Θ_B (meV)	Θ_p (meV)	Θ_r (meV)	p	Δp	ρ	$\Delta\rho$
0.00	2.6	7.8	4.2	12.0	37.3	19.9	2.24	0.50	0.49	0.43
0.05	2.7	4.1	3.5	11.7	18.0	16.3	2.40	0.46	0.44	0.40
0.11	2.8	3.6	3.4	12.3	14.7	15.5	2.63	0.41	0.35	0.36
0.14	3.0	4.3	3.8	12.7	16.7	16.5	2.59	0.42	0.34	0.35
0.23	3.1	4.5	4.1	13.8	17.2	18.0	2.71	0.40	0.30	0.33
0.27	3.0	3.9	3.8	14.7	15.8	18.1	2.92	0.36	0.23	0.29
0.35	3.2	4.1	3.9	14.0	15.6	17.4	2.82	0.38	0.26	0.31

masses, $\hbar\omega_{\mathrm{LO}}$ is the LO-phonon energies, $\Omega = L_xL_yL_z$ is the volume of the sample, and q ($(q = q_x, q_y, n\pi/L_z)$, for n integer) is the phonon wavevector. In the $Al_xGa_{1-x}As$ alloy, the electron and hole effective masses, the LO-phonon energies, and the term $(1/\varepsilon_\infty - 1/\varepsilon_s)$ increase with the Al concentration, leading to an increase of the electron–LO-phonon coupling with x in GaAs/$Al_xGa_{1-x}As$ QWs. The mean energy of the TO ($\langle\hbar\omega_{\mathrm{LO}}\rangle$) and LO ($\langle\hbar\omega_{\mathrm{TO}}\rangle$) phonons, described by Θ_B, also increases with x [30].

The parameter p can be analyzed using equation (3) where ω_0 is the cutoff frequency and can be determined by the fitting procedure using the relation $\hbar\omega_0 = [(\nu+1)/\nu]k_B\Theta_p = [p/(p-1)]k_B\Theta_p$ with $p = \nu + 1$. We observe in our results that the value of the cutoff energy decreases in going from the bulk ($x = 0.0$) to the quantum well (with $x = 0.05$) and oscillates around 25–27 meV. Among other factors, the spectral function changes by increasing x due to the development of an energy gap in the phonon spectra. The parameter p, which mimics the true dependence on energy of the density of states (DOS), will also depend on x. There are two possible explanations for the change of the parameter p. The first is that the energies of the peaks of the DOS do not change but their intensities change with x. The second alternative is that the energies of the peaks in the DOS increase, but their intensities

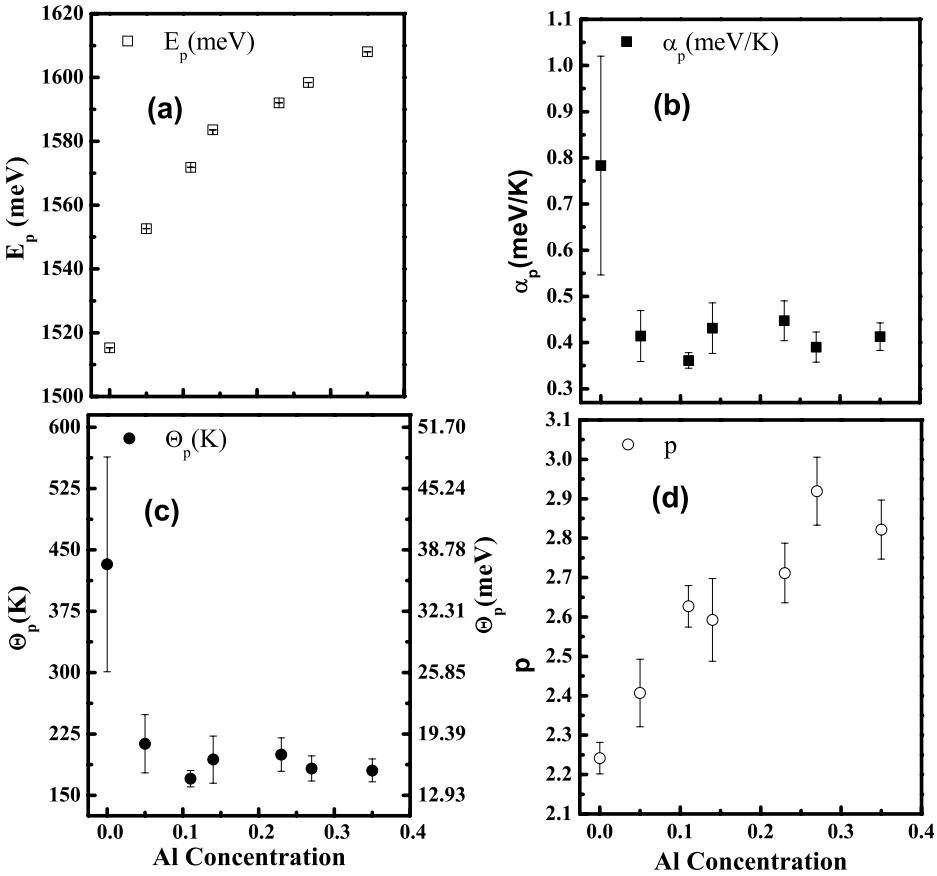

Figure 4. Dependence on aluminum concentration of the fitted parameters according to the p-type Pässler model for the temperature range $9 \leqslant T \leqslant 100$ K.

do not change. In both cases the parameter p will increase with x and it is not possible to conclude which effect leads to the pattern observed for the parameter p in figure 4. However, since the optical phonon energies increase by increasing x, it is reasonable to expect that the intensity and energy of the LO-phonons at the GaAs/AlGaAs interfaces will also depend on x and that both effects will contribute to the increase of p by increasing the alloy composition.

In the analysis of the behavior of the ρ-parameter with the aluminum concentration, we must take into account two important effects: (i) that the energy of the optical phonons increases with the Al concentration, and (ii) that an energy gap between the maximum energy of the acoustic branches and the minimum energy of the optical branches develops by increasing the alloy concentration. In the same temperature range (9–100 K), the separation between acoustical and optical phonon branches increases leading to a decrease of their probability of excitation. However, this effect is probably less efficient than the increase of the vibrational mean energy, resulting in an increase of the ρ-parameter with Al concentration which means an increase of the electron–optical phonon interaction. Since the α-parameter is also related to the strength of the electron–phonon interaction, α_p increases and ρ decreases by increasing x.

The three parameters Θ_B, $\Theta_{\rm p}$, and Θ_r (or α_B, α_p, and α_ρ) can be analyzed together since they have the same physical meaning. In order to analyze each ternary of parameters, we show in figure 6 the values of the parameters obtained for the QWs normalized with respect to the correspondent bulk values. We can see in this figure that, in general, the α_B and Θ_B parameters obtained with the Viña model have a higher value when compared to the bulk values. The parameters obtained according to the p-type model (α_p and $\Theta_{\rm p}$) have values smaller than the bulk parameters. The parameters of the ρ-type model (α_ρ and Θ_r) have intermediary values (between the values of the Viña and p-type models).

The effective energy of the acoustic phonons obtained by the two Pässler models, $\Theta_{\rm p}$ and Θ_r, is almost constant with respect to x with a mean value given by $\langle\Theta_{\rm p}\rangle_x \approx \langle\Theta_r\rangle_x = 16.5$ meV, a value which is located with respect to the energy scale approximately in the middle of the acoustic phonon branch ($\varepsilon_{\rm LA} = 29/2 \approx 14.5$ meV). The acoustic phonon energies display a very weak dependence on the alloy concentration as can be observed in figure 6 by the behavior of the Θ parameters of the Pässler models.

Our findings also show that the confinement leads to a decrease of the interaction between electrons and acoustic phonons. This interaction is described by the equivalent parameter a_B of the Pässler models: $a_p = \alpha_p\Theta_{\rm p}/2$ and $a_\rho = \alpha_\rho\Theta_\rho/2$. Since the parameters $\Theta_{\rm p}$, Θ_ρ are approximately constants for $x \geqslant 0.05$, the electron–phonon interaction will be mainly described by the α_p (or α_ρ). It is obvious that the

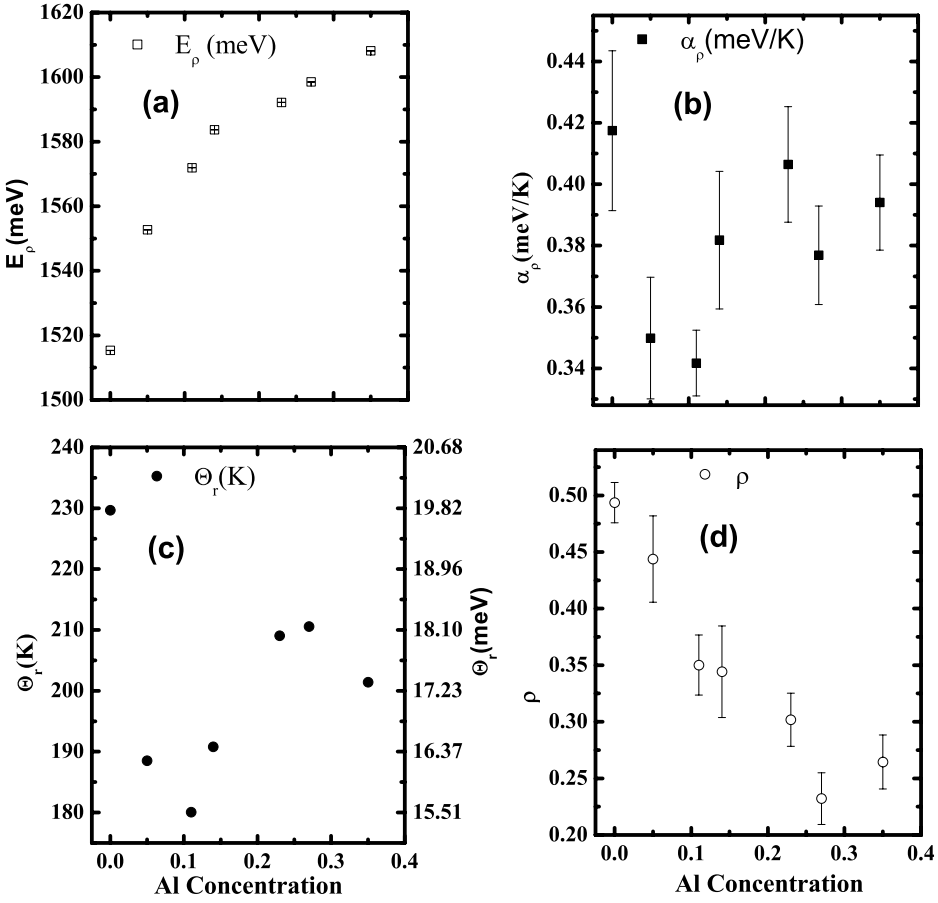

Figure 5. Dependence on aluminum concentration of the fitted parameters according to the ρ-type Pässler model for the temperature range $9 \leqslant T \leqslant 100$ K.

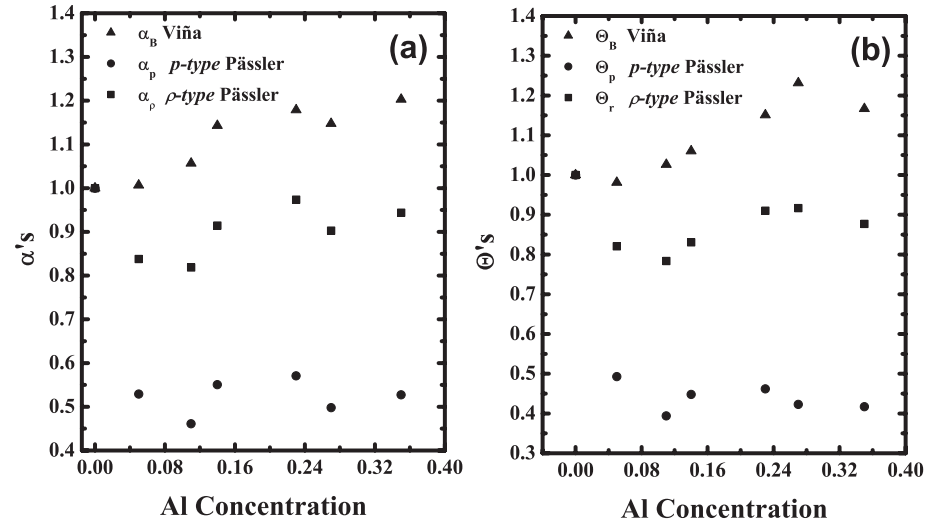

Figure 6. Dependence on aluminum concentration of the fitting parameters normalized with respect to the bulk value, obtained according to the different theoretical models and valid for the temperature range $9 \leqslant T \leqslant 100$ K.

quantitative analysis of this parameter is not reliable due to the small temperature range used in our experiments, but it is possible to do a comparative analysis of the data.

The analysis of our results shows that the parameter α_p, which describes primarily the acoustic phonon interaction, is constant for the complete aluminum concentration range here analyzed. However, since the ρ-type model mainly describes the optical phonons ($\rho < 0.5$), the obtained values of α_ρ show a dependence with the alloy concentration, even in the small range of temperatures here analyzed (i.e. small value of T_{cutoff}).

Our findings obtained by the analysis of dependence of the energy gap on temperature are similar to the results obtained by Rudin *et al* [23, 31] by analyzing the half-width at half-maximum (HWHM) of the excitonic emissions. For semiconductor bulk materials and heterostructures, the contribution of the exciton–acoustic phonon interaction to the HWHM is the sum of the contributions of the deformation potential (DP) and the piezoelectric (PE) interaction and can be described by the following expression: $\Gamma = \Gamma(0) + \Gamma^{DP} + \Gamma^{PE} = \Gamma(0) + a_{ph}T$ where $\Gamma(0)$ denotes the temperature-independent part and $a_{ph} = \Gamma^{DP}/T + \Gamma^{PE}/T$ (in μeV K^{-1}) describes the strength of the electron–acoustic phonon interaction [31]. As discussed by Rudin *et al* [31] each term Γ^{DP}/T and Γ^{PE}/T is concomitantly related to the conduction band (CB) and valence band (VB). As a consequence, the exciton radius and the conduction and valence band anisotropies in reciprocal space are fundamentals to estimate the contribution of each term to the parameter a_{ph} describing the electron–acoustic phonon interaction. For materials and heterostructures with isotropic CB and VB, the DP contribution is prevalent while the PE contribution is negligible. However, for systems with anisotropic conduction and valence bands, the PE contribution can be very significant. For instance, the dispersion relation of the heavy-hole exciton in bulk GaAs is strongly anisotropic, resulting in a PE contribution of approximately 85% while only 15% comes from the DP interaction [31]. Moreover, several experimental results for the HWHM obtained by different techniques show that the electron–acoustic phonon interaction has values in the range 1–3 μeV K^{-1} [20–22, 25, 32] for QWs with well widths smaller than 200 Å, while for GaAs bulk the values are in the range 8–12 μeV K^{-1} [20, 23], which shows that the electron–phonon interaction is approximately five times weaker in GaAs/Al$_x$Ga$_{1-x}$As quantum wells than in GaAs bulk.

By analyzing the exciton–acoustic phonon scattering process in QWs, we notice that the symmetry is reduced and the degeneracy of the valence band at the center of the Brillouin zone is partially lifted, leading to a reduction of the anisotropy. Thus, we can consider that in quantum wells the PE contribution can be disregarded as compared to the DP contribution. That being the case, we can say that the appearance of a discrete set of energy levels (due to the confinement by the introduction of the barriers) leads to a decrease of the exciton–acoustic phonon interaction when the system undergoes a change from the 3D (GaAs bulk) to the 2D (GaAs/Al$_x$Ga$_{1-x}$As QW) confinement conditions [19]. Therefore, the fitting models of $E_g(T)$ that present more susceptibility to the electron–acoustic phonon interaction at low temperatures ($T < 100$ K)—the p-type followed by the ρ-type—must provide the best description of the influence of the confinement effects on the fitting parameters when the system undergoes the 3D-to-2D transition.

Finally, besides the fact that the values of the parameters obtained for the QWs (see figure 6) are always smaller when compared to the respective bulk values, it is possible to observe a common behavior in all data determined by using the three different models: an oscillation as a function of the alloy concentration. According to Iotti *et al* [33], this oscillation can be related to the change of the oscillator strength of the excitonic radiative recombination as the exciton wavefunction spreads through the barriers. Systematic calculations about the oscillator strength for GaAs/GaAlAs quantum wells with specific configurations (alloy concentration and well width) are required in order to verify this statement.

5. Conclusion

In the present paper we have investigated the dependence on composition of the energy band-gaps of GaAs/AlGaAs quantum wells using photoluminescence experiments. The behavior of the experimental excitonic transition energy as a function of temperature was analyzed using three different theoretical models. Our findings show that the values of the fitted parameters also depend on the barrier material (AlGaAs) and not only on the well material (GaAs). The comparison of the results for the GaAs bulk material (3D system) with the results obtained for the QWs (2D systems) shows that: (i) the model of Viña does not describe the exciton confinement and the electron–acoustic phonon interaction; (ii) the p-type model has more susceptibility to the quantum confinement effect and to the electron–acoustic phonon interaction, exhibiting a behavior similar to the dependence on temperature of the half-width at half-maximum measured by several other experimental techniques; the ρ-type model describes more precisely the effect of the exciton confinement and contemplates the relative weight of the electron–optical/acoustic phonon interaction. The effect of the confinement was clearly observed in the abrupt drop of the values of the fitted parameters α_p and α_ρ, Θ_p and Θ_r. Finally, we also verified that the p-type model provides the best fit to the experimental data, with the smallest values of S^2.

Acknowledgments

The authors would like to acknowledge the financial support granted by the following Brazilian agencies: Coordenação de Aperfeiçoamento de Pessoal de Nível Superior (CAPES), Conselho Nacional de Desenvolvimento Científico e Tecnológico (CNPq), Fundação Araucária de Apoio ao Desenvolvimento Científico e Tecnológico do Paraná (Fundação Araucária), and Fundação Banco do Brasil (FBB).

References

[1] Cardona M 2004 *Phys. Rev. Lett.* **92** 196403
[2] Debye P 1907 *Ann. Phys.* **22** 180
[3] Pässler R 1999 *Phys. Status Solidi* b **216** 975
[4] Allen P B and Heine V 1976 *J. Phys. C: Solid State Phys.* **9** 2305
[5] Lourenço S A, Dias I F L, Duarte J L, Laureto E, Poças L C, Toginho Filho D O and Leite J R 2004 *Braz. J. Phys.* **34** 517
[6] Zollner S, Gopalan S and Cardona M 1991 *Solid. State Commun.* **77** 485
[7] Allen P B and Cardona M 1981 *Phys. Rev.* B **23** 1495
[8] Manoogian A and Wolley J C 1984 *Can. J. Phys.* **62** 285
[9] Walter J P, Zucca R R L, Cohen M L and Shen Y R 1970 *Phys. Rev. Lett.* **24** 102

[10] Manoogian A and Leclerc A 1979 *Phys. Status Solidi* b **92** K23
[11] Viña L, Logothetidis S and Cardona M 1984 *Phys. Rev.* B **30** 1979
[12] Pässler R 1997 *Phys. Status Solidi* b **200** 155
Pässler R and Oelgart G 1997 *J. Appl. Phys.* **82** 2611
[13] Varshni Y P 1967 *Physica (Utrecht)* **34** 194
[14] Logothetidis S, Cardona M and Garriga M 1991 *Phys. Rev.* B **43** 11950
[15] Lourenço S A, Dias I F L, Laureto E, Duarte J L, Meneses E A, Leite J R and Mazzaro I 2001 *J. Appl. Phys.* **89** 6159
[16] Lourenço S A, Dias I F L, Duarte J L, Laureto E, Toginho Filho D O, Meneses E A and Leite J R 2001 *Eur. Phys. J.* B **21** 11
[17] Lourenço S A, Dias I F L, Duarte J L, Laureto E, Iwamoto H, Meneses E A and Leite J R 2001 *Superlatt. Microstruct.* **29** 225
[18] Daly E M, Glynn T J, Lambkin J D, Considine L and Walsh S 1995 *Phys. Rev.* B **52** 469
[19] Rudin S and Reinecke T L 2002 *Phys. Rev.* B **65** 121311
[20] Schulteis L, Honold A, Kuhl J, Köhler K and Tu C W 1986 *Phys. Rev.* B **34** 9027
[21] Gammon D, Rudin S, Reinecke T L, Katzer D S and Kyono C S 1995 *Phys. Rev.* B **51** 16785
[22] Borri P, Langbein W, Hvam J M and Martilli F 1999 *Phys. Rev.* B **59** 2215
[23] Rudin S, Reinecke T L and Segall B 1990 *Phys. Rev.* B **42** 11218
[24] Ruf T, Spitzer J, Belitskj V F, Cardona M and Ploog K 1994 *Phys. Rev.* B **50** 1792
[25] Srinivas S, Hryniewicz J, Chen Y J and Wood C E C 1992 *Phys. Rev.* B **46** 10193
[26] Pässler R 1998 *J. Appl. Phys.* **83** 3356
[27] Lourenço S A, da Silva M A T, Dias I F L, Duarte J L, Laureto E, Quivy A A and Lamas T E 2007 *J. Appl. Phys.* **101** 113536
[28] Hirakawa K and Sakuki H 1986 *Appl. Phys. Lett.* **49** 889
[29] Bastard G, Mendez E E, Chang L L and Esaki L 1982 *Phys. Rev.* B **26** 1974
[30] Adachi S 1982 *J. Appl. Phys.* **53** 5683
[31] Rudin S and Reinecke T L 2002 *Phys. Rev.* B **66** 085314
[32] Baroni S, Gironcoli S and Giannozzi P 1990 *Phys. Rev. Lett.* **65** 84
[33] Iotti R C and Andreani L C 1997 *Phys. Rev.* B **56** 3922